REVISITING THE LOWER BOUND ON TIDAL DEFORMABILITY DERIVED BY AT 2017GFO

Kenta Kiuchi[1,2], Koutarou Kyutoku[3,4,5,2], Masaru Shibata[1,2], Keisuke Taniguchi[6]
Draft version March 12, 2019

ABSTRACT

We revisit the lower bound on binary tidal deformability $\tilde{\Lambda}$ imposed by a luminous kilonova/macronova, AT 2017gfo, by numerical-relativity simulations of models consistent with gravitational waves from the binary-neutron-star merger, GW170817. Contrary to the claim made in the literature, we find that binaries with $\tilde{\Lambda} \lesssim 400$ can explain the luminosity of AT 2017gfo as far as moderate mass ejection from the remnant is assumed as also done in the previous work. The reason is that the maximum mass of a neutron star is not strongly correlated with tidal deformability of neutron stars with typical mass of $\approx 1.4 M_\odot$. If the maximum mass is so large that the binary does not collapse to a black hole immediately after merger, the mass of the ejecta can be sufficiently large irrespective of the binary tidal deformability. We explicitly present models of binary mergers with $\tilde{\Lambda}$ down to 242 that satisfy the requirement on the mass of the ejecta from the luminosity of AT 2017gfo. We further find that the luminosity of AT 2017gfo could even be explained by models that do not experience bounce after merger. We conclude that the luminosity of AT 2017gfo is not very useful to constrain the binary tidal deformability. Accurate estimation of the mass ratio will be necessary to put a lower bound using electromagnetic counterparts in the future. We also caution that merger simulations performed employing a limited class of tabulated equations of state could be severely biased due to the lack of generality.

Keywords: stars: neutron — equation of state — gravitational waves

1. INTRODUCTION

The first binary-neutron-star merger was observed as a multi-messenger event GW170817/GRB 170817A/AT 2017gfo (Abbott et al. 2017c,b,d). Gravitational and electromagnetic signals have been combined to derive various information about physics and astrophysics. Examples include the velocity of gravitational waves (Abbott et al. 2017b), Hubble's constant (Abbott et al. 2017a), the central engine of (a kind of) short gamma-ray bursts (Mooley et al. 2018), and the origin of (at least a part of) r-process elements (Kasen et al. 2017; Tanaka et al. 2017).

The multi-messenger observations also constrain properties of neutron stars. Gravitational waves, GW170817, constrain the so-called binary tidal deformability to $100 \lesssim \tilde{\Lambda} \lesssim 800$, where precise values depend on the method of analysis and adopted theoretical waveforms (De et al. 2018; Abbott et al. 2018, 2019). At the same time, various researchers argue that the maximum mass of a neutron star $M_{\max}$ cannot be significantly larger than ≈ 2.15–$2.2 M_\odot$ based on the electromagnetic features, e.g. the absence of magnetar-powered radiation

(Margalit & Metzger 2017; Shibata et al. 2017; Rezzolla et al. 2018; Ruiz et al. 2018). Bauswein et al. (2017) also propose lower bounds on the radii of massive neutron stars assuming that the electromagnetic signals may imply avoidance of the prompt collapse. These inferences imply that supranuclear-density matter is unlikely to be very stiff.

Radice et al. (2018b) proposed a novel idea that $\tilde{\Lambda} \gtrsim 400$ is required to eject material heavier than $0.05 M_\odot$, which they assumed to be required by high luminosity of AT 2017gfo.[7] The logic is that no binary model with $\tilde{\Lambda} \lesssim 400$ is capable of ejecting $0.05 M_\odot$, even if all the baryonic remnant can be ejected, in their numerical-relativity simulations performed with four tabulated equations of state derived by mean-field theory. This constraint approximately indicates that neutron stars must be larger than $12\,\mathrm{km}$ (Zhao & Lattimer 2018), and thus it could reject mildly soft equations of state if reliable. Indeed, this constraint has been used to infer properties of nuclear matter by various researchers (Most et al. 2018; Lim & Holt 2018; Malik et al. 2018; Burgio et al. 2018). Later Radice & Dai (2018) and Coughlin et al. (2018b) derived a slightly weak bound on the value of $\tilde{\Lambda}$ by statistical inferences based on modified assumptions, but the logic is essentially the same as they rely on the same simulations.

Tews et al. (2018) critically examined this idea by using parameterized, general nuclear-matter equations of state. Their key finding is that the maximum mass is correlated only very weakly with binary tidal deformability for the masses consistent with GW170817. They found that some equations of state can support a neutron star with $> 2.6 M_\odot$ even if $\tilde{\Lambda}$ is significantly lower than 400.

[1] Max Planck Institute for Gravitational Physics (Albert Einstein Institute), Am Mühlenberg 1, Potsdam-Golm 14476, Germany
[2] Center for Gravitational Physics, Yukawa Institute for Theoretical Physics, Kyoto University, Kyoto, 606-8502, Japan
[3] Theory Center, Institute of Particles and Nuclear Studies, KEK, Tsukuba 305-0801, Japan
[4] Department of Particle and Nuclear Physics, the Graduate University for Advanced Studies (Sokendai), Tsukuba 305-0801, Japan
[5] Interdisciplinary Theoretical and Mathematical Sciences Program (iTHEMS), RIKEN, Wako, Saitama 351-0198, Japan
[6] Department of Physics, University of the Ryukyus, Nishihara, Okinawa 903-0213, Japan

[7] Precisely, this threshold is derived by fitting the multi-color evolution of AT 2017gfo.

Because the remnant massive neutron star should survive very long or possibly permanently after merger for these cases (Hotokezaka et al. 2011, 2013a), the argument of Radice et al. (2018b) based on the mass of the ejecta cannot reject such equations of state and then binary tidal deformability. However, the maximum mass of a neutron star might also be constrained to $\lesssim 2.2 M_\odot$ as described above. Whether this constraint on the maximum mass is compatible with the luminosity of AT 2017gfo is not trivial.

In this paper, we demonstrate that the lower bound on $\tilde{\Lambda}$ is not as significant as that Radice et al. (2018b) proposed even if the maximum mass is only moderately large, $M_{\mathrm{max}} \lesssim 2.1 M_\odot$, by a suite of numerical-relativity simulations. Specifically, we find that various models with $\tilde{\Lambda} < 400$ can eject $0.05 M_\odot$ and can explain the luminosity of AT 2017gfo. The models include asymmetric binary neutron stars with $\tilde{\Lambda} = 242$, which may not collapse at least until 20 ms after merger. In addition, we also show that the luminosity of AT 2017gfo could be explained even if the merger remnant does not experience bounce after merger when the binary is asymmetric.

2. MODEL AND EQUATION OF STATE

We simulate mergers of equal-mass binaries with $1.375 M_\odot$–$1.375 M_\odot$ and unequal-mass binaries with $1.2 M_\odot$–$1.55 M_\odot$. The total mass, $2.75 M_\odot$, and the mass ratios, $q = 1$ or 0.774, are consistent with GW170817 (Abbott et al. 2017c, 2019) and also with observed Galactic binary neutron stars (e.g. Tauris et al. 2017; Ferdman & PALFA Collaboration 2018). This should be contrasted with Radice et al. (2018b), where many models are significantly heavier than GW170817, particularly those with $\tilde{\Lambda} \lesssim 400$, and the mass ratio is restricted to $q > 0.857$. The initial orbital angular velocity Ω of the binary is chosen to be $G m_0 \Omega / c^3 \approx 0.025$ with applying eccentricity reduction (Kyutoku et al. 2014), where G and c are the gravitational constant and the speed of light, respectively. The binaries spend about six orbits before merger.

Equations of state for neutron-star matter are varied systematically by adopting piecewise polytropes with three segments (Read et al. 2009). This choice allows us to investigate more generic models than particular nuclear-theory models, e.g. mean-field theory. The low-density segment is identical to that adopted in Hotokezaka et al. (2011). The middle-density segment is specified by pressure at $10^{14.7} \,\mathrm{g\,cm^{-3}}$ denoted by $P_{14.7}$ and an adiabatic index Γ. This segment is matched to the low-density part at the density where the pressure equals. The value of $P_{14.7}$ is known to be correlated with the neutron-star radius (Lattimer & Prakash 2001; Read et al. 2009), and we choose $\log P_{14.7} \,(\mathrm{dyne\,cm^{-2}})$ from $\{34.1, 34.2, 34.3, 34.4, 34.5\}$. The value of Γ is determined by, in conjunction with the high-density segment, requiring the maximum mass of neutron stars to become $2.00 M_\odot$, $2.05 M_\odot$, and $2.10 M_\odot$. The high-density segment is given by changing the adiabatic index to 2.8 at $10^{15} \,\mathrm{g\,cm^{-3}}$.

First two columns of Table 1 list Γ and $P_{14.7}$ for the fourteen[8] equations of state adopted in this study. The

radius of a $1.35 M_\odot$ neutron star and the maximum mass are shown in the third and fourth columns, respectively. We checked that all of them are causal, i.e. the sound velocity does not exceed c, up to the central density of the spherical maximum-mass configuration.

Table 1 also presents the binary tidal deformability of our equal-mass and unequal-mass binaries in the sixth column, where the mass ratio is given in the fifth column. All are consistent with constraints obtained by GW170817 irrespective of the details of the analysis (Abbott et al. 2017c; De et al. 2018; Abbott et al. 2018, 2019). As pointed out by Tews et al. (2018), the binary tidal deformability is not directly correlated with the maximum mass.

3. METHOD OF SIMULATIONS

Numerical simulations are performed in full general relativity with the SACRA code (Yamamoto et al. 2008; Kiuchi et al. 2017). The finite-temperature effect is incorporated by an ideal-gas prescription following Hotokezaka et al. (2011) with the fiducial value of $\Gamma_{\mathrm{th}} = 1.8$, which may be appropriate for capturing the dynamics of remnant neutron stars (Bauswein et al. 2010). We also performed simulations with $\Gamma_{\mathrm{th}} = 1.5, 1.6$, and 1.7 for some models with low values of $\tilde{\Lambda}$, and dependence of our results on Γ_{th} will be discussed. Because whether the merger remnant collapses to a black hole in a short time scale or not is important for this study, detailed physical effects such as magnetic fields and neutrino transport are neglected. They are known to play a central role on a longer time scale than durations of our simulations, which are performed until 10–20 ms after merger (Hotokezaka et al. 2013a), and thus our results should depend only weakly on these effects. Although we cannot determine the electron fraction of the ejecta, which is important to derive nucleosynthetic yields and characteristics of the kilonova/macronova (Wanajo et al. 2014; Tanaka et al. 2017; Kasen et al. 2017), it is not relevant to the purpose of this work.

We classify the fate of merger remnants into three types. If the remnant collapses to a black hole without experiencing bounce after merger, we call it a no-bounce collapse. Note that such collapses are denoted by the prompt collapse in Bauswein et al. (2017), but we avoid this name taking into account the fact that some asymmetric models survive longer than the dynamical time scale up to a few ms even if they do not experience bounce. If the remnant evades the no-bounce collapse but still collapses in the duration of our simulations, specifically by 10–20 ms after merger, it is regarded as a short-lived remnant. This time scale is approximately identical to that adopted in Radice et al. (2018b). If the remnant massive neutron star does not collapse in our simulations, it is called a long-lived remnant. These three types will be denoted by "no bounce", "short", and "long" in Table 1, respectively.

We derive the baryonic mass of the unbound dynamical ejecta, M_{dyn}, and that of the bound material outside the black hole, M_{bd}, from the simulations. The ejecta as a whole should consist of the dynamical ejecta and the late-time outflow from the merger remnant (e.g. Fernández & Metzger 2013; Metzger & Fernández 2014;

---

[8] We do not adopt $(\log P_{14.7}, M_{\mathrm{max}}) = (34.5, 2.1 M_\odot)$, because

it turned out to be unnecessary for our purpose.

Table 1

Characteristic quantities of equations of state adopted in this work and results of simulations. The first and second columns show the parameters that specify an equation of state, Γ and $\log P_{14.7}$, respectively. The third and fourth columns show the radius of a $1.35 M_\odot$ neutron star $R_{1.35}$ and the maximum mass $M_{\max}$, respectively. The next five columns present models of binaries and results of simulations, where the upper and lower rows correspond to equal-mass and unequal-mass binaries, respectively. The values of the mass ratio q and binary tidal deformability $\tilde{\Lambda}$ are given in the fifth and sixth columns, respectively. The seventh, eighth, and ninth columns show the fate of the remnant, the mass of dynamical ejecta M_{dyn}, and the mass of the bound material outside the black hole M_{bd}, for our fiducial $\Gamma_{\mathrm{th}} = 1.8$. The fate is classified into the collapse without bounce (no bounce), the short-lived remnant (short), and the long-lived remnant (long) as defined in the body text. The mass of the remnant is not shown for the long-lived cases.

Γ	$\log P_{14.7}$ (dyne cm^{-2})	$R_{1.35}$ (km)	$M_{\max}$ [$M_\odot$]	q	$\tilde{\Lambda}$	type	M_{dyn} [$M_\odot$]	M_{bd} [$M_\odot$]
3.765	34.1	10.4	2.00	1	208	no bounce	$< 10^{-3}$	$< 10^{-3}$
				0.774	218	no bounce	$< 10^{-3}$	0.023
3.887	34.1	10.5	2.05	1	221	no bounce	$< 10^{-3}$	$< 10^{-3}$
				0.774	230	no bounce	5.2×10^{-3}	0.029
4.007	34.1	10.5	2.10	1	232	no bounce	1.9×10^{-3}	2.7×10^{-3}
				0.774	242	long	0.013	—
3.446	34.2	10.6	2.00	1	232	no bounce	$< 10^{-3}$	$< 10^{-3}$
				0.774	245	no bounce	2.3×10^{-3}	0.036
3.568	34.2	10.7	2.05	1	247	no bounce	$< 10^{-3}$	$< 10^{-3}$
				0.774	259	no bounce	0.014	0.038
3.687	34.2	10.8	2.10	1	260	short	1.4×10^{-3}	7.8×10^{-3}
				0.774	272	long	0.011	—
3.132	34.3	11.0	2.00	1	272	no bounce	$< 10^{-3}$	$< 10^{-3}$
				0.774	290	no bounce	0.012	0.063
3.252	34.3	11.1	2.05	1	288	no bounce	1.2×10^{-3}	1.9×10^{-3}
				0.774	305	short	0.015	0.12
3.370	34.3	11.1	2.10	1	303	short	1.9×10^{-3}	0.031
				0.774	319	long	0.011	—
2.825	34.4	11.6	2.00	1	345	short	6.5×10^{-3}	0.018
				0.774	373	short	0.011	0.087
2.942	34.4	11.6	2.05	1	362	short	2.5×10^{-3}	0.016
				0.774	387	short	0.011	0.12
3.058	34.4	11.6	2.10	1	377	long	9.7×10^{-3}	—
				0.774	400	long	9.0×10^{-3}	—
2.528	34.5	12.5	2.00	1	508	short	9.4×10^{-3}	0.053
				0.774	558	short	5.6×10^{-3}	0.16
2.640	34.5	12.4	2.05	1	516	short	0.012	0.12
				0.774	560	long	6.3×10^{-3}	—

Just et al. 2015; Fujibayashi et al. 2018). Because our simulations do not include magnetic fields or corresponding viscosity required to launch the outflow, we simply assume that some fraction of M_{bd} will be ejected by such processes following Radice et al. (2018b). While Radice et al. (2018b) conservatively (for their purpose) adopted 100% efficiency for the ejection from the accretion torus, this efficiency is likely to be lower than 50%, particularly when the remnant is a black hole, because the outflow is a result of the accretion. If the remnant is long-lived, we simply consider that the ejecta can be sufficiently massive to explain the luminosity of AT 2017gfo. This is consistent with the result of Radice et al. (2018b), where the analysis was made based on the material with its rest-mass density being below $10^{13}\,\mathrm{g\,cm^{-3}}$.

Our results depend weakly on grid resolutions. By simulating selected models with three different resolutions, we estimate that the mass of the ejecta has a relative error of about a factor of two and an absolute error of $10^{-3} M_\odot$ for typical cases with hypothetical first-order convergence. However, the nominal error reaches an order of magnitude for marginally stable short-lived remnants, because the fate wanders from the no-bounce collapse to the short-lived remnant. We think that this is reasonable and inevitable for models near the threshold, and these errors should be kept in mind when we discuss implications to AT 2017gfo. It is encouraging that no long-lived remnant changes its fate for different grid resolutions, and thus our long-lived remnants may safely be regarded as being capable of explaining the luminosity of

AT 2017gfo. In this paper, we only show the results of highest-resolution runs, in which the neutron-star radius is covered by ≈ 65–70 points with ≈ 120–$150\,\mathrm{m}$ spacings.

4. RESULT

The merger of binary neutron stars results in dynamical mass ejection and formation of a remnant, a massive neutron star or a black hole, surrounded by an accretion torus. Because their dynamics and mechanisms have thoroughly been described in previous publications (e.g. Hotokezaka et al. 2013b; Bauswein et al. 2013; Radice et al. 2016), we do not repeat detailed explanations. The fate of the merger remnant (seventh), the mass of the dynamical ejecta (eighth), and the mass of the bound material outside the black hole (ninth) are presented in Table 1. The mass of the bound material, M_{bd}, for a given equation of state is always larger for unequal-mass binaries than for equal-mass binaries because of efficient tidal interaction and angular momentum transfer during merger. In particular, some of the asymmetric models leave a baryonic mass of $\gtrsim 0.03 M_\odot$ even for the no-bounce collapse. This is because the light components are deformed significantly before merger and the collapses are gradually induced by the accretion for these models (see http://www2.yukawa.kyoto-u.ac.jp/~kenta.kiuchi/GWRC/index.html for visualization).

The masses of the ejecta are summarized visually in Fig. 1 against the binary tidal deformability, $\tilde{\Lambda}$. It is obvious that many binary models with $\tilde{\Lambda} < 400$ can eject
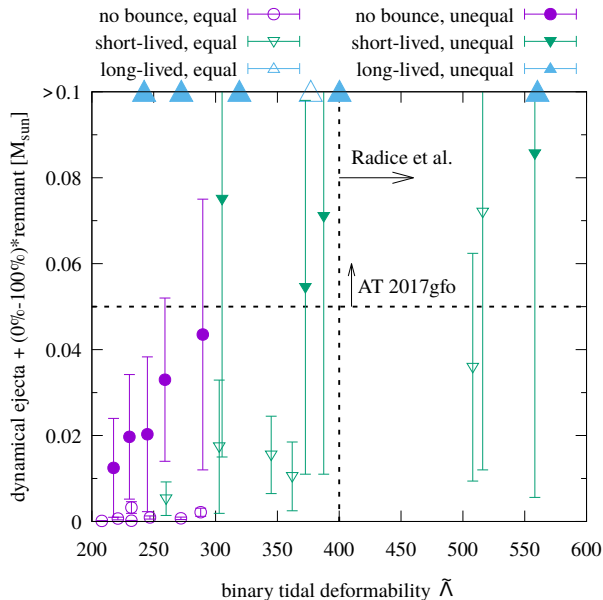
Figure 1. Mass of the ejecta versus the binary tidal deformability. The errorbars indicate ejection of the remnant by from 0% (i.e. only dynamical mass ejection occurs) to 100% (i.e. all the mass outside the black hole is ejected), and the 50% ejection of the baryonic mass surrounding the black hole is marked with symbols. Open and filled symbols denote equal-mass and unequal-mass models, respectively. Large triangles on the top axis denote the models for which remnant massive neutron stars survive longer than 10–20 ms and thus the luminosity of AT 2017gfo can be explained. Such a model is found even at $\tilde{\Lambda} = 242$. The vertical dashed line at $\tilde{\Lambda} = 400$ is the threshold proposed by Radice et al. (2018b). The horizontal dashed line at $0.05 M_{\odot}$ indicates the mass required to explain AT 2017gfo (Radice et al. 2018b).

more than $0.05 M_{\odot}$ and are capable of explaining the luminosity of AT 2017gfo as far as the mass of the ejecta is concerned. Indeed, we find that a handful of binary models with $\tilde{\Lambda} < 400$ result in formation of a long-lived remnant. They serve as counterexamples to the claim that $\tilde{\Lambda} \gtrsim 400$ is required to explain AT 2017gfo (Radice et al. 2018b).

The key ingredients are the not-so-small maximum mass, $M_{\max}$, and the mass asymmetry represented by the small mass ratio, q. Their importance is understood from Fig. 2, where we summarize which model can explain the luminosity of AT 2017gfo in the $\tilde{\Lambda}$-$M_{\max}$ plane. Here, we assume 50% ejection efficiency of the bound material for concreteness. On one hand, for the case that the maximum mass is $2 M_{\odot}$, all the models collapse by 10–20 ms after merger. Not only equal-mass models have no chance of ejecting $0.05 M_{\odot}$,[9] but also the mass asymmetry of $q = 0.774$ does not save any model with $\tilde{\Lambda} < 377$. On the other hand, if the maximum mass is as large as $2.1 M_{\odot}$, many models produce long-lived remnants. Actually, all the asymmetric binaries considered here result in forming the long-lived remnants and thus are capable of explaining the luminosity AT 2017gfo. The lowest value of $\tilde{\Lambda}$ of models that can eject $0.05 M_{\odot}$ is 242. Figure 2 suggests that, if $M_{\max}$ is larger than $2.1 M_{\odot}$, the lower bound on $\tilde{\Lambda}$ derived by AT 2017gfo may become looser than that found in this study.

[9] A model with $\tilde{\Lambda} = 508$ can eject $0.05 M_{\odot}$ if the efficiency exceeds 90%.
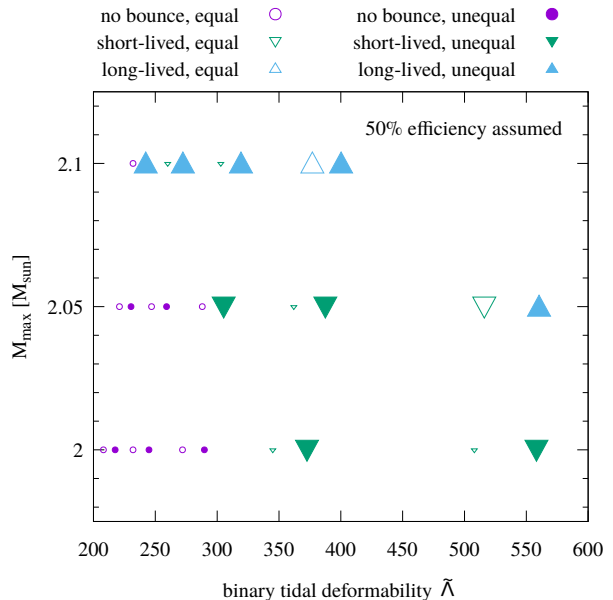

Figure 2. Summary of whether the luminosity of AT 2017gfo can be explained by each model in the binary tidal deformability ($\tilde{\Lambda}$)-maximum mass ($M_{\max}$) plane. The large symbols denote models that can eject $0.05 M_{\odot}$ with hypothetical 50% efficiency and can explain the luminosity of AT 2017gfo, and the small ones denote those cannot.

We also find that all the models with $\tilde{\Lambda} > 400$ are capable of ejecting $0.05 M_{\odot}$ if 100% ejection efficiency is adopted. This is consistent with the finding of Radice et al. (2018b).

The fate of the merger remnant depends on the strength of the finite-temperature effect for marginal cases. For example, the lowest value of $\tilde{\Lambda}$ that can explain the luminosity of AT 2017gfo is 242 in our models if the fiducial $\Gamma_{\mathrm{th}} = 1.8$ is adopted, where the outcome is a long-lived remnant. However, the remnant becomes short lived for $\Gamma_{\mathrm{th}} \leq 1.7$ because of the reduced thermal pressure and fails to eject $0.05 M_{\odot}$. This indicates that the finite-temperature effect must be moderately strong for this model to account for AT 2017gfo. We also find that the model with $\tilde{\Lambda} = 272$ results in the long-lived remnant only when $\Gamma_{\mathrm{th}} \geq 1.6$, whereas the short-lived remnant for a very small value of $\Gamma_{\mathrm{th}} = 1.5$ can eject $0.05 M_{\odot}$ if 100% efficiency is assumed. Although our conclusion that binaries with $\tilde{\Lambda} \lesssim 400$ are capable of explaining the luminosity of AT 2017gfo is unchanged, these observations imply that accurate incorporation of the finite-temperature effect is also crucial to infer precise properties of the zero-temperature equation of state from electromagnetic counterparts.

5. DISCUSSION

We conclude that the lower bound on binary tidal deformability is $\tilde{\Lambda} \leq 242$ if ejection of $0.05 M_{\odot}$ is required. We speculate that lower values of $\tilde{\Lambda}$ than this could even be acceptable if we employ an equation of state that supports the maximum mass larger than $2.1 M_{\odot}$ and/or increase the degree of asymmetry. The precise value of the threshold depends also on the strength of the finite-temperature effect, represented by Γ_{th} in our study.

We also find that an asymmetric binary that results

in a no-bounce collapse can explain the luminosity of AT 2017gfo, if moderately high $\approx 60\%$ ejection efficiency from the remnant is admitted. The lower bounds proposed in Bauswein et al. (2017) are satisfied for the equation of state of this model, with which the radii of $1.6 M_\odot$ and maximum-mass configurations are 10.93 and 9.66 km, respectively. However, our finding would potentially invalidate the argument of Bauswein et al. (2017) and its future application.

Our results indicate that the mass ratio is critically important to derive reliable constraints on neutrons-star properties from electromagnetic emission as also argued in Radice et al. (2018b). If the binary turns out to be symmetric, it is possible that $\tilde{\Lambda} \gtrsim 400$ is necessary as Radice et al. (2018b) originally proposed. Indeed, we find no symmetric model with $\tilde{\Lambda} < 377$ that can eject $0.05 M_\odot$. Further investigation is required to clarify precisely the effect of asymmetry. Although the mass ratio can be determined from gravitational-wave data analysis, the degeneracy with the spin must be resolved to achieve high precision (Hannam et al. 2013).

The velocity and the composition can potentially be used as additional information to examine binary models. Some previous work tried to associate either the blue or red component of AT 2017gfo to dynamical ejecta to improve parameter estimation (Gao et al. 2017; Coughlin et al. 2018a). However, the derived binary parameters, in particular the mass ratio, disagree between these work. As shown by Kawaguchi et al. (2018), such an association is not necessarily justified once interaction among multiple ejecta components is taken into account. Detailed modelings of the emission are required if we would like to utilize the velocity and/or the composition to put constraints on properties of neutron stars.

Another lesson drawn from our study is that the possible parameter space of nuclear physics may not be satisfactorily covered by current tabulated equations of state (Tews et al. 2018). For example, equations of state derived by relativistic mean-field theory tend to predict a large maximum mass only when the typical radius is large (Radice et al. 2018a), and thus the value of binary tidal deformability is also high. Such a correlation is not likely to be physical but ascribed to the method of quantum many-body calculations. Specifically, the large maximum mass and the small radius can be accommodated in variational calculations (e.g. Togashi et al. 2017). As Fig. 2 shows, the outcome of merger depends significantly on the maximum mass even if the binary tidal deformability is unchanged. It should be remarked that models with $\tilde{\Lambda} < 400$ of Radice et al. (2018b) are generated by assigning total masses larger than those allowed by GW170817 (Abbott et al. 2017c, 2019) except for the SFHo equation of state (Steiner et al. 2013). It is impossible for other equations of state adopted by them to produce binary models equipped with $\tilde{\Lambda} \lesssim 400$ and the total mass allowed by GW170817 simultaneously. This feature artificially enhances the chance of the early collapse. If we wish to put reliable constraints on neutron stars via numerical simulations, care must be taken regarding the limitation of the adopted models including the finite-temperature effect.

REFERENCES

Abbott, B. P., et al. 2017a, Nature, 551, 85
—. 2017b, ApJ, 848, L13
—. 2017c, Phys. Rev. Lett., 119, 161101
—. 2017d, ApJ, 848, L12
—. 2018, Phys. Rev. Lett., 121, 161101
—. 2019, Phys. Rev. X, 9, 011001
Bauswein, A., Goriely, S., & Janka, H.-T. 2013, ApJ, 773, 78
Bauswein, A., Janka, H.-T., & Oechslin, R. 2010, Phys. Rev. D, 82, 084043
Bauswein, A., Just, O., Janka, H.-T., & Stergioulas, N. 2017, ApJ, 850, L34
Burgio, G. F., Drago, A., Pagliara, G., Schulze, H.-J., & Wei, J.-B. 2018, ApJ, 860, 139
Coughlin, M. W., et al. 2018a, MNRAS, 480, 3871
Coughlin, M. W., Dietrich, T., Margalit, B., & Metzger, B. D. 2018b, arXiv:1812.04803
De, S., Finstad, D., Lattimer, J. M., Brown, D. A., Berger, E., & Biwer, C. M. 2018, Phys. Rev. Lett., 121, 091102
Ferdman, R. D., & PALFA Collaboration. 2018, in IAU Symposium, Vol. 337, Pulsar Astrophysics the Next Fifty Years, ed. P. Weltevrede, B. B. P. Perera, L. L. Preston, & S. Sanidas, 146–149
Fernández, R., & Metzger, B. D. 2013, MNRAS, 435, 502
Fujibayashi, S., Kiuchi, K., Nishimura, N., Sekiguchi, Y., & Shibata, M. 2018, ApJ, 860, 64
Gao, H., Cao, Z., Ai, S., & Zhang, B. 2017, ApJ, 851, L45
Hannam, M., Brown, D. A., Fairhurst, S., Fryer, C. L., & Harry, I. W. 2013, ApJ, 766, L14
Hotokezaka, K., Kiuchi, K., Kyutoku, K., Muranushi, T., Sekiguchi, Y.-i., Shibata, M., & Taniguchi, K. 2013a, Phys. Rev. D, 88, 044026
Hotokezaka, K., Kiuchi, K., Kyutoku, K., Okawa, H., Sekiguchi, Y.-i., Shibata, M., & Taniguchi, K. 2013b, Phys. Rev. D, 87, 024001
Hotokezaka, K., Kyutoku, K., Okawa, H., Shibata, M., & Kiuchi, K. 2011, Phys. Rev. D, 83, 124008
Just, O., Bauswein, A., Pulpillo, R. A., Goriely, S., & Janka, H.-T. 2015, MNRAS, 448, 541
Kasen, D., Metzger, B., Barnes, J., Quataert, E., & Ramirez-Ruiz, E. 2017, Nature, 551, 80
Kawaguchi, K., Shibata, M., & Tanaka, M. 2018, ApJ, 865, L21
Kiuchi, K., Kawaguchi, K., Kyutoku, K., Sekiguchi, Y., Shibata, M., & Taniguchi, K. 2017, Phys. Rev. D, 96, 084060
Kyutoku, K., Shibata, M., & Taniguchi, K. 2014, Phys. Rev. D, 90, 064006
Lattimer, J. M., & Prakash, M. 2001, ApJ, 550, 426
Lim, Y., & Holt, J. W. 2018, Phys. Rev. Lett., 121, 062701
Malik, T., et al. 2018, Phys. Rev. C, 98, 035804
Margalit, B., & Metzger, B. D. 2017, ApJ, 850, L19
Metzger, B. D., & Fernández, R. 2014, MNRAS, 441, 3444
Mooley, K. P., et al. 2018, Nature, 561, 355
Most, E. R., Weih, L. R., Rezzolla, L., & Schaffner-Bielich, J. 2018, Phys. Rev. Lett., 120, 261103
Radice, D., & Dai, L. 2018, arXiv:1810.12917
Radice, D., Galeazzi, F., Lippuner, J., Roberts, L. F., Ott, C. D., & Rezzolla, L. 2016, MNRAS, 460, 3255
Radice, D., Perego, A., Hotokezaka, K., Fromm, S. A., Bernuzzi, S., & Roberts, L. F. 2018a, ApJ, 869, 130
Radice, D., Perego, A., Zappa, F., & Bernuzzi, S. 2018b, ApJ, 852, L29
Read, J. S., Lackey, B. D., Owen, B. J., & Friedman, J. L. 2009, Phys. Rev. D, 79, 124032

Rezzolla, L., Most, E. R., & Weih, L. R. 2018, ApJ, 852, L25

Ruiz, M., Shapiro, S. L., & Tsokaros, A. 2018, Phys. Rev. D, 97, 021501

Shibata, M., Fujibayashi, S., Hotokezaka, K., Kiuchi, K., Kyutoku, K., Sekiguchi, Y., & Tanaka, M. 2017, Phys. Rev. D, 96, 123012

Steiner, A. W., Hempel, M., & Fischer, T. 2013, ApJ, 774, 17

Tanaka, M., et al. 2017, PASJ, 69, 102

Tauris, T. M., et al. 2017, ApJ, 846, 170

Tews, I., Margueron, J., & Reddy, S. 2018, Phys. Rev. C, 98, 045804

Togashi, H., Nakazato, K., Takehara, Y., Yamamuro, S., Suzuki, H., & Takano, M. 2017, Nucl. Phys. A, 961, 78

Wanajo, S., Sekiguchi, Y., Nishimura, N., Kiuchi, K., Kyutoku, K., & Shibata, M. 2014, ApJ, 789, L39

Yamamoto, T., Shibata, M., & Taniguchi, K. 2008, Phys. Rev. D, 78, 064054

Zhao, T., & Lattimer, J. M. 2018, Phys. Rev. D, 98, 063020